Isolated RNA Binding Domain of a Class I tRNA Synthetase†

Andrew J. Gale and Paul Schimmel*

Department of Biology, Massachusetts Institute of Technology, Cambridge, Massachusetts 02139

Received March 27, 1995; Revised Manuscript Received May 8, 1995®

ABSTRACT: Class I tRNA synthetases typically have two major domains consisting of a class-defining N-terminal nucleotide binding fold, which contains the active site, and an idiosyncratic C-terminal domain, which in many instances provides for interactions with the tRNA anticodon. Whether the C-terminal domain can function in specific RNA binding when disconnected from the catalytic core is not known. We fused the anticodon binding domain of *Escherichia coli* methionyl tRNA synthetase to maltose binding protein. This fusion protein and the released, isolated domain are stable and have native-like structural characteristics, as shown by circular dichroism and thermal denaturation studies. Both the fusion protein and the isolated domain bind specifically to a small RNA hairpin oligonucleotide that recapitulates the anticodon stem−loop of $tRNA^{fMet}$. Neither protein binds to an RNA hairpin with a point mutation in the anticodon trinucleotide. The binding specificity and affinity of these proteins duplicate those of the interaction between methionyl tRNA synthetase and the anticodon stem−loop oligonucleotide. Thus, the anticodon binding domain is functionally independent of the class-defining catalytic core and can be joined to another protein with little change in RNA binding characteristics.

The aminoacyl tRNA synthetase family of proteins provides the enzymatic basis for the genetic code by catalyzing the aminoacylation of transfer RNAs with their cognate amino acid. The synthetases are classified into two groups of ten enzymes each on the basis of conserved sequence motifs that correspond to specific three-dimensional structural elements (Webster et al., 1984; Hountondji et al., 1986; Ludmerer & Schimmel, 1987; Cusack et al., 1990; Eriani et al., 1990; Burbaum & Schimmel, 1991b). Methionyl tRNA synthetase (MetRS)[1] is included in the class I enzymes, which are defined by the presence of a conserved 11-amino acid signature sequence (Webster et al., 1984) that ends in the HIGH tetrapeptide and by the KMSKS pentapeptide (Hountondji et al., 1986). Both of these sequence elements are found in the N-terminal catalytic domain, which forms a topologically conserved structure built around a Rossman nucleotide binding fold.

All tRNAs adopt a similar L-shaped tertiary structure that has two domains. One consists of the acceptor stem and the TΨC-stem and loop and the other consists of the D-stem and loop and the anticodon stem and loop (Figure 1). Aminoacyl tRNA synthetases in both classes contain nonconserved domains in addition to the conserved active site domains. A common theme among the aminoacyl tRNA synthetases is that the conserved catalytic domain interacts with the tRNA acceptor−TΨC helix and a second nonconserved domain interacts with regions of the tRNA distal to the acceptor stem. This second domain provides for interactions with the tRNA anticodon in many instances (Perona et al., 1991; Rould et al., 1991; Cavarelli et al., 1993; Kim et al., 1993a).

Three groups have independently proposed that the two major domains of transfer RNAs had separate origins (Maizels & Weiner, 1993; Noller, 1993; Schimmel et al., 1993). In particular, the acceptor−TΨC stem−loop minihelix is thought to be the original substrate for aminoacylation, with the anticodon-containing domain being added later as a template "reading head". The ability of at least eight different synthetases to aminoacylate minihelix substrates with a high degree of RNA sequence specificity demonstrates an RNA−amino acid relationship that is distinct from the trinucleotide−amino acid relationships of the genetic code (Schimmel et al., 1993).

The class-defining catalytic core of synthetases is believed to be the historical enzyme that carried out amino acid activation and had polypeptide insertions that enabled it to bind to and aminoacylate RNA substrates based on the acceptor−TΨC stem−loop minihelix (Buechter & Schimmel, 1993a). The second major domain has been proposed to be fused to progenitor aminoacyl tRNA synthetases at the time when the second, anticodon-containing domain of tRNAs was added (Buechter & Schimmel, 1993a; Schimmel et al., 1993). In the case of MetRS, the class-defining catalytic domain is within the N-terminal half of the structure. The C-terminal domain is predominantly α-helical, and this domain contains residues that interact directly with the anticodon of $tRNA^{Met}$ (Valenzuela & Schulman, 1986; Ghosh et al., 1990, 1991; Meinnel et al., 1991b; Kim et al., 1993a). Previous work demonstrated that MetRS could be split so that the two domains of the synthetase were expressed as separate polypeptides. A noncovalent complex of these two domains maintained high levels of activity (Burbaum & Schimmel, 1991a). This finding showed that the function of the combined domains is independent of a covalent connection between them.

†This work was supported by Grant Number GM 15539 from the National Institutes of Health. A.J.G. was a predoctoral trainee of the National Institutes of Health (1992−1994) and was supported by a National Science Foundation Graduate Fellowship (1989−1992).

* Author to whom correspondence should be addressed.

® Abstract published in *Advance ACS Abstracts,* June 15, 1995.

[1] Abbreviations: MetRS, methionyl tRNA synthetase; MBP, maltose binding protein; IPTG, isopropyl 1-thio-β-D-galactopyranoside; EDTA, ethylenediaminetetraacetic acid; β-ME, β-mercaptoethanol; PMSF, phenylmethanesulfonyl fluoride; PEI, poly(ethyleneimine); BSA, bovine serum albumin; SDS−PAGE, sodium dodecyl sulfate−polyacrylamide gel electrophoresis; CD, circular dichroism.

0006-2960/95/0434-8896$09.00/0

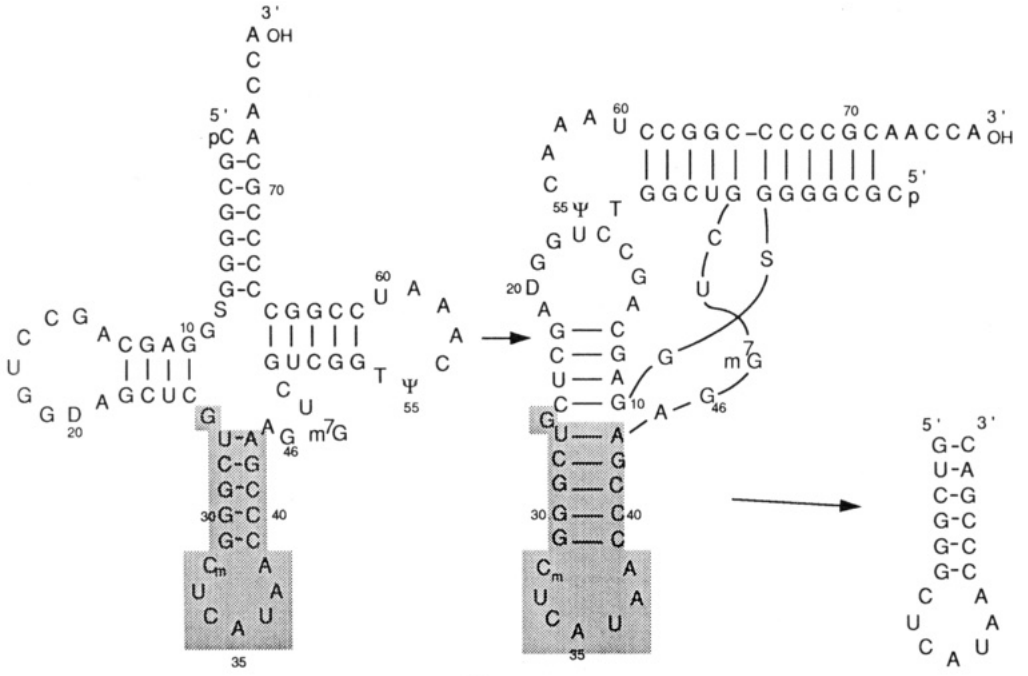

FIGURE 1: Sequence and cloverleaf structure of *E. coli* $tRNA^{fMet}$ (left) (Sprinzl et al., 1989), the L-shaped arrangement of the three-dimensional structure (center), and the sequence and hairpin structure of the anticodon stem−loop RNA substrate (right). The hairpin structure is based on the shaded portion, to which a C was added to the 3′-end to pair with the unmatched G.

Based on this previous work, and considering the pathways for the evolution of the two-domain structure of tRNA synthetases, we considered whether the anticodon binding domain could function as a discrete unit when joined to an arbitrary protein. In particular, a peptide "appendix" at the end of the anticodon binding domain curls back to the active site of the N-terminal domain of MetRS, thereby linking together the two structures (Brunie et al., 1990; Kim et al., 1993b). We thought that this linkage, as well as the packing interaction of the domain interface, might be necessary to achieve a conformation for RNA binding by the C-terminal domain.

In this work, we fused amino acids 367−547 of the anticodon binding domain with maltose binding protein (MBP) (Guan et al., 1987; Maina et al., 1988). We also released the anticodon binding domain by proteolytic cleavage. This fusion protein (MBP−$C_{367-547}$) and the C-terminal domain ($C_{367-547}$) itself were physically characterized and the RNA binding function was investigated by affinity coelectrophoresis (ACE) (Lee & Lander, 1991). This method enabled us to detect directly RNA−protein complexes formed with a small RNA hairpin oligonucleotide that recapitulates the anticodon stem−loop of $tRNA^{fMet}$.

MATERIALS AND METHODS

Construction and Purification of Fusion Proteins. Phagemid pJB104 encodes the monomeric form of *Escherichia coli* methionyl tRNA synthetase (residues 1−547) (Kim & Schimmel, 1992). (All work in this paper was done with the 547-amino acid N-terminal fragment of MetRS, which hereafter will simply be referred to as $MetRS_{1-547}$.) Site-directed mutagenesis with the Sculptor *in vitro* mutagenesis system (Amersham, Arlington Heights, IL) was used to insert a *Bam*HI site in the $MetRS_{1-547}$ gene of phagemid pJB104 directly before the codon for I367. The mutagenic primer, 5′-CGATATCATCAATGGATCCAGAGAGTTTCGC-3′, was used for this purpose. This construct (plasmid pAG117) was cleaved with *Bam*HI to produce a 759-base pair fragment that was inserted into the *Bam*HI site of plasmid pMal-c2 (New England Biolabs, Inc., Beverly, MA) (Guan et al., 1987; Maina et al., 1988) to produce a gene fusion between *MalE* and codons 367−547 of MetRS. The resulting plasmid is designated as pAG120 (Figure 2).

Plasmid pAG120 was transformed into *E. coli* strain TG1 *(SupE hsdΔ5 thi Δ(lac-proAB) F′[traD36 proAB+ lacI^q lacZΔM15])*. Expression of MBP−$C_{367-547}$ was induced with 0.5 mM IPTG, and the cells were harvested at late log phase. Cells were resuspended in buffer containing 20 mM Tris-HCl (pH 7.5), 200 mM NaCl, 1 mM EDTA, 10 mM β-ME, and 0.5 mM PMSF and lysed in a French press at 15 000 lbs/in.^{2}. The lysate was centrifuged at 27000*g* for 15 min, and the resulting supernatant was precipitated with 0.2% PEI and then centrifuged at 12000*g* for 10 min. The supernatant was then dialyzed into 25 mM Tris-HCl (pH 7.5) and 1 mM β-ME. MBP−$C_{367-547}$ in this solution was purified using an FPLC system with a Mono Q HR 10/10 column (Pharmacia LKB Biotechnology, Uppsala, Sweden) with a linear NaCl gradient from 0 to 400 mM. Fractions containing fusion protein were identified by SDS−PAGE, concentrated to about 20 mg/mL protein, and then purified using an FPLC Superose 12 column (Pharmacia LKB Biotechnology, Uppsala, Sweden) in 25 mM Tris-HCl (pH 7.5), 200 mM NaCl, and 1 mM β-ME. Protein concentration was determined by absorbance at 280 nm (Edelhoch, 1967; Cassio & Waller, 1971).

$MetRS_{1-547}$ was produced from a high-expression construct made by inserting the MetRS gene from the phagemid pJB104 into the plasmid pKK223-3 expression vector with its *tac* promoter (Pharmacia Biotech, Inc., Piscataway, NJ). Phagemid pJB104 was cleaved with *Eco*RI and *Sal*I, plasmid pKK223-3 was cleaved with *Eco*RI, and both were digested with mung bean nuclease to remove single-stranded ends (Sambrook et al., 1989). The $MetRS_{1-547}$ gene was blunt-end-ligated (Sambrook et al., 1989) into plasmid pKK223-3

to produce plasmid pAG112. $MetRS_{1-547}$ was purified as described earlier for the fusion protein, except that after PEI precipitation the supernatant was fractionated with ammonium sulfate, and proteins precipitated at 30−55% ammonium sulfate were resuspended in 25 mM Tris-HCl (pH 7.5) and 1 mM β-ME. This solution was then dialyzed into the same buffer to remove ammonium sulfate and purified by FPLC as described earlier for MBP−$C_{367-547}$.

Cleavage of MBP−$C_{367-547}$. MBP−$C_{367-547}$ was cleaved using factor X_a (New England Biolabs, Inc., Beverly, MA) in 50 mM Tris-HCl (pH 7.5), 100 mM NaCl, and 2 mM $CaCl_2$. MBP−$C_{367-547}$ at a concentration of 1 mg/mL was incubated with factor X_a at a concentration of 5 μg/mL (200:1, w:w) for 12 h at room temperature. This reaction was then dialyzed into 25 mM Tris-HCl (pH 7.5) and 1 mM β-ME, and domain $C_{367-547}$ was separated from maltose binding protein by anion exchange using a Mono Q HR 10/10 column (Pharmacia LKB Biotechnology, Uppsala, Sweden) as described earlier.

Circular Dichroism Spectroscopy. CD experiments were performed on an AVIV Model 62DS CD spectrometer with an AVIV Model W5TE-159-S thermoelectric temperature-controlled cuvette holder (AVIV Associates, Inc., Lakewood, NJ). All experiments were done in 20 mM sodium phosphate (pH 7.3), 100 mM NaCl, and 1 mM β-ME. Spectra were recorded from 260 to 200 nm in 1 nm wavelength increments, with a signal acquired for 5 s at each wavelength with a 1.5 nm bandwidth. The signal was recorded in units of mean residue ellipticity ($[\theta]$, deg cm^2 dmol^{-1}). Thermal denaturation was monitored by the change in $[\theta]$ at 222 nm. Temperature was incremented in 1 °C steps from 25 to 80 °C. The samples were equilibrated for 1 min at each temperature, and the signal was recorded for 5 s. The pH of the buffer in this temperature range changed by less than 0.2 pH unit. The melting temperature was determined as the minimum of the first derivative of $[\theta]$ at 222 nm versus 1/temperature (Cantor & Schimmel, 1980b). All spectra and thermal denaturation experiments were done at both 50 μg/mL protein and 1 mg/mL protein with a 5 mm path length and a 0.5 mm path length, respectively.

Synthesis and Radioactive Labeling of RNA Oligonucleotides. RNA oligonucleotides were chemically synthesized on a Gene Assembler Plus synthesizer (Pharmacia LKB Biotechnology Inc., Piscataway, NJ) as previously described (Usman et al., 1987; Scaringe et al., 1990; Musier-Forsyth et al., 1991). The RNA substrate was 5′-^{32}P-labeled according to Silberklang et al. (1977) and Park and Schimmel (1988).

Affinity Coelectrophoresis. Affinity coelectrophoresis was used to investigate the binding of the proteins to the RNA substrates. Affinity coelectrophoresis is a technique that was developed by Lee and Lander (1991) to investigate the binding of proteins to glycosaminoglycans under equilibrium conditions. It is also generally applicable to protein−nucleic acid binding interactions (Lim et al., 1991), and it is particularly useful for visualizing the relatively weak binding interactions of aminoacyl tRNA synthetases with their cognate tRNAs and tRNA fragments (Kim et al., 1993b).

Custom gel electrophoresis equipment for these experiments was made by Owl Scientific (Cambridge, MA). Low melting point agarose (LMP agarose) (BRL, Gaithersburg, MD) (1%) was prepared in 50 mM Hepes (pH 7.5), 0.1 mM EDTA, 4 mM $MgCl_2$, 1 mM β-ME, and 100 μg/mL BSA. A Teflon comb with 10 parallel bars that have a footprint of 35 × 2 mm and are separated from each other by 5 mm was placed on Gelbond film (FMC Bioproducts, Rockland, ME) in a Plexiglas casting tray. A Teflon comb that made a well measuring 73 × 1 mm was placed 4 mm from one end of the parallel bars. The agarose was poured to a depth of about 2 mm. When the combs were removed, 10 parallel 35 × 2 mm wells perpendicular to a 73 × 1 mm slot resulted. The appropriate protein was then prepared in a series of concentrations in buffer at twice the desired final concentrations. These samples were mixed 1:1 with 2% LMP agarose and loaded into the 35 × 2 mm wells.

The [5′-^{32}P]RNA (10 000−50 000 cpm) was diluted to 70 μL (to a final concentration of roughly 10 nM) in the buffer described earlier along with 0.02% bromophenol blue, 0.02% xylene cyanol, and 3% glycerol and then loaded into the 73 × 1 mm slot. The gel was electrophoresed at 150 V for 1.5−2 h in a thermostated circulating gel box (Hoefer Super Sub Model HE100, Hoefer Scientific, San Francisco, CA) at 25 °C. The gel running buffer was the gel buffer without β-ME and BSA. Gels were dried in an open vacuum oven with low heat and visualized using a phosphorimager from Molecular Dynamics (Sunnyvale, CA).

The [5′-^{32}P]RNA was electrophoresed most of the way through the protein in each lane. The K_d was determined by measuring the vertical shift m of [^{32}P]RNA in each protein lane, relative to a protein-free lane. This shift should be proportional to the fraction of RNA bound to protein at equilibrium in the gel, assuming that the kinetics of association and dissociation are rapid relative to electrophoresis times and that there are only two states, bound and free (Lim et al., 1991). The shift value m was divided by the maximal possible shift n to give a retardation coefficient R ($R = m/n$). A Scatchard plot of R versus $R/[\text{protein}_{tot}]$ gives a linear plot whose slope is equal to $-1/K_d$ (Lim et al., 1991).

RESULTS

Production and Cleavage of MBP−$C_{367-547}$. We chose the maltose binding protein (MBP) to fuse to the anticodon binding domain of MetRS. This protein has a molecular weight of 42 500, and its interaction with amylose can be used as a basis to purify a fusion protein. In addition, the use of a linker with a factor X_a cleavage site enables the release of the polypeptide joined to MBP. The fusion protein MBP−$C_{367-547}$ was expressed at high levels in *E. coli* strain TG1, typically yielding 40 mg/L culture. The expressed fusion protein was soluble and stable and therefore amenable to purification (data not shown). We attempted to purify this protein with an amylose resin column (Maina et al., 1988), but although this column bound MBP with high affinity, MBP−$C_{367-547}$ did not bind well to the amylose resin. Instead, we used ion exchange chromatography on a Mono Q HR 10/10 column followed by gel filtration on Superose 12, which yielded MBP−$C_{367-547}$ of about 90% purity (Figure 3).

Factor X_a at a 1:200 (w:w) ratio cleaved 100% of the fusion protein, and domain $C_{367-547}$ was then separated from MBP by ion exchange chromatography on a Mono Q HR 10/10 column (Figure 3). Edman degradation of the released cleavage product (carried out by the MIT Biopolymers Laboratory) verified that the N-terminus had the sequence ISEFGSIDDI, as expected (Figure 2). Although purified

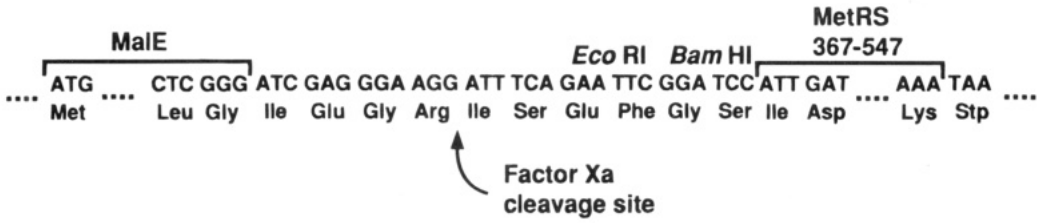

FIGURE 2: Diagrammatic representation of the coding sequence of the junction between MBP and domain $C_{367-547}$ in the gene for fusion protein MBP$-C_{367-547}$. A *Bam*HI site was added to the $MetRS_{1-547}$ gene in phagemid pJB104. A *Bam*HI fragment was then excised from plasmid pJB104 and inserted into the *Bam*HI site of plasmid pMal-c2 to give plasmid pAG120.

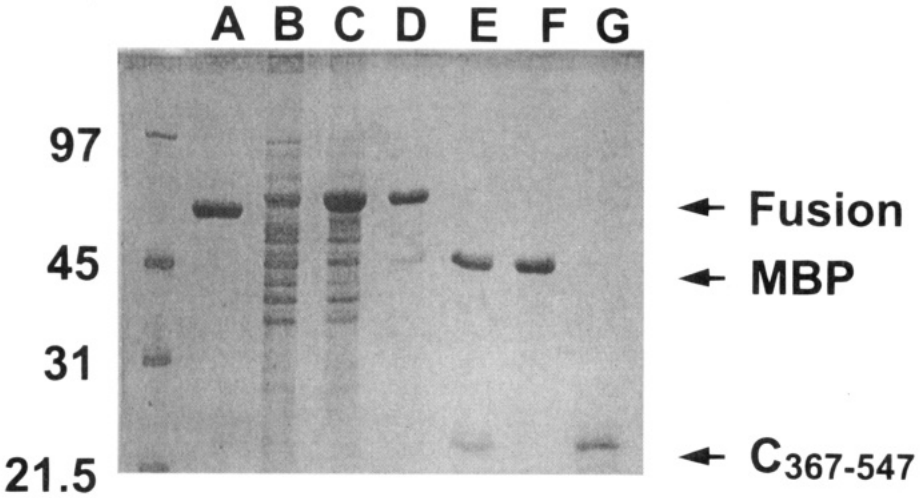

FIGURE 3: SDS−PAGE of extracts of cells expressing MBP$-C_{367-547}$ and purification and cleavage of MBP$-C_{367-547}$. Left lane: molecular weight standards with molecular weights (×1000) given along the left ordinate. (A) $MetRS_{1-547}$; (B) 7.5 μg of protein from extracts of uninduced pAG120/TG1 cells; (C) 7.5 μg of protein from extracts of pAG120/TG1 cells induced to express MBP$-C_{367-547}$ at mid-log phase for 4 h with 0.5 mM IPTG; (D) 3 μg of MBP$-C_{367-547}$; (E) 5 μg of MBP$-C_{367-547}$ cleaved with factor X_a; (F) 3 μg of MBP cleaved from MBP$-C_{367-547}$ and purified from $C_{367-547}$; (G) 3 μg of $C_{367-547}$ cleaved from MBP$-C_{367-547}$ and purified from MBP.

domain $C_{367-547}$ was analyzed by circular dichroism, amounts of cleaved domain $C_{367-547}$ sufficient to analyze for RNA binding by affinity coelectrophoresis (>5 mg) were limited. This limitation is primarily due to the relatively high levels of expensive factor X_a needed to cleave the fusion protein. Therefore, most of the affinity coelectrophoresis analyses were done with the intact fusion protein MBP$-C_{367-547}$.

Circular Dichroism and Thermal Melting Curves. According to the X-ray crystal structure of $MetRS_{1-547}$ (Brunie et al., 1990), the secondary structure of domain $C_{367-547}$ is primarily α-helical. Domain $C_{367-547}$ has a CD spectrum similar to that of $MetRS_{1-547}$, with minima at 209 and 222 nm (Figure 4A). These minima are characteristic of α-helix secondary structure (Cantor & Schimmel, 1980a). The similarities of the CD spectra of the two proteins suggest that domain $C_{367-547}$ has a native structure like that of the same domain contained in the intact protein. The contribution of the N-terminal domain of MetRS to the CD spectrum decreases the negative peaks at 209 and 222 nm because that domain has short elements of β-strand, α-helix, and irregular structures, which *in toto* should reduce the overall signal when expressed in units of mean residue ellipticity (Cantor & Schimmel, 1980a).

We also compared the CD spectrum of domain $C_{367-547}$ to spectra of MBP$-C_{367-547}$ and MBP alone (data not shown). Both domains are primarily α-helical and show characteristic minima at 209 and 222 nm. However, the CD spectrum of MBP alone has an overall minimum at 222 nm, whereas domain $C_{367-547}$ has a global minimum at 209 nm. Domain $C_{367-547}$ also has a deeper minimum with a value of −16 500 deg cm^2 dmol^{-1} at 209 nm, whereas MBP has a value of −11 000 deg cm^2 dmol^{-1} at 222 nm. The spectrum for MBP$-C_{367-547}$ falls between these two spectra and qualitatively appears to be an average of the combined spectra (data not shown). The spectra for $MetRS_{1-547}$, $C_{367-547}$, and MBP$-C_{367-547}$ all show some dependence on concentration, with all three showing somewhat less α-helical character at 50 μg/mL than at 1 mg/mL. MBP, however, was entirely concentration-independent. These results suggest that there is little difference between the overall structure of domain $C_{367-547}$ in the fusion protein and as an "isolated protein".

Thermal melting curves of domain $C_{367-547}$ were performed to evaluate the thermal stability of this domain relative to intact $MetRS_{1-547}$ and to fusion protein MBP$-C_{367-547}$ (Figure 4B). Thermal denaturation was monitored at the 222 nm local minimum characteristic of α-helix structure. Experiments were done at both 50 μg/mL and 1 mg/mL for all proteins. $MetRS_{1-547}$ and MBP$-C_{367-547}$ had similar denaturation profiles at 1 mg/mL, where $MetRS_{1-547}$ had an apparent T_m of 61.5 °C and MBP$-C_{367-547}$ had an apparent T_m of 63 °C (Figure 4B).

In both cases denaturation was not reversible, probably because of the aggregation of denatured protein. Denaturation of the fusion protein was somewhat concentration-dependent with an apparent T_m of 56 °C at 50 μg/mL. It was not possible to measure the apparent T_m of $MetRS_{1-547}$ at 50 μg/mL because the denatured protein appeared to precipitate out of solution and settle to the bottom of the cuvette. However, the denaturation transition of $MetRS_{1-547}$

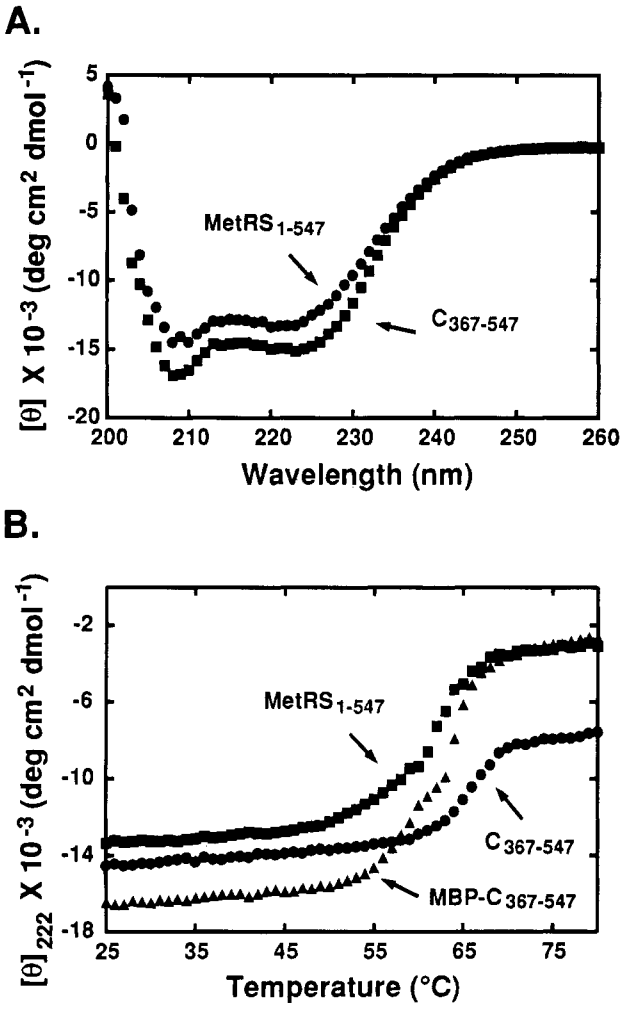

FIGURE 4: Circular dichroism analysis of $C_{367-547}$. (A) CD spectra of $MetRS_{1-547}$ and $C_{367-547}$ at 25 °C on an AVIV 62DS CD spectrometer, each at a concentration of 1 mg/mL. (B) Thermal denaturation curves of $MetRS_{1-547}$, $C_{367-547}$, and MBP–$C_{367-547}$, each at a concentration of 1 mg/mL. All CD spectra and thermal denaturation curves were done in 20 mM sodium phosphate (pH 7.3), 100 mM NaCl, and 1 mM β-ME.

at 50 μg/mL appeared to start at the same temperature as $MetRS_{1-547}$ at 1 mg/mL.

The thermal denaturation curve of domain $C_{367-547}$ consistently showed a sharp cooperative transition, but the measured apparent T_m's varied significantly from preparation to preparation (Figure 4B). This variation was probably due to differences in the trace amounts of undigested MBP–$C_{367-547}$ and smaller fragments of $C_{367-547}$ present in purified preparations of $C_{367-547}$. In all cases, the denaturation was largely nonreversible and aggregation was observed after denaturation. In four experiments with four independent preparations of $C_{367-547}$, apparent T_m's ranged from 62 to 68 °C at 1 mg/mL protein and from 60 to 67.5 °C at 50 μg/mL. The denaturation curve shown in Figure 4B has an apparent T_m of 66 °C.

Although some aggregation during the thermal denaturation of these proteins was evident, the cooperativity of the transitions (Figure 4B) suggests a native-like structure for the C-terminal domain, both independently and as part of the fusion protein MBP–$C_{367-547}$. $C_{367-547}$ appears to be as stable as, or more stable than, $MetRS_{1-547}$ or MBP–$C_{367-547}$.

Affinity Coelectrophoresis. Affinity coelectrophoresis is a gel retardation method in which the protein of interest is imbedded directly in an agarose gel at defined concentrations (see Materials and Methods) The labeled RNA substrate is then electrophoresed through the protein in the gel, which allows the measurement of binding affinities under equilibrium conditions (Lee & Lander, 1991; Lim et al., 1991; Kim et al., 1993b). As seen in Figure 5A, labeled anticodon stem–loop RNA (Figure 1) is retarded to a position higher in the gel as the MetRS concentration increases. This retardation produces a binding isotherm from which a dissociation constant can be calculated using a Scatchard plot (see Materials and Methods).

We found that, with this assay, $MetRS_{1-547}$ binds to $tRNA^{fMet}$ with a K_d of 3.6 μM at pH 7.5 and 25 °C (data not shown). By using the same procedure, the dissociation constant for the anticodon stem–loop RNA (Figure 1) was 31 ± 5 μM (Table 1). (By using an anticodon stem–loop structure as a competitive inhibitor of aminoacylation, Meinnel et al. (1991a) obtained a K_I = 38 ± 5 μM at pH 7.6 and 25°C.) The 8–9-fold difference between the dissociation constant for $tRNA^{fMet}$ and that for the anticodon stem–loop suggests that much of the binding energy between $MetRS_{1-547}$ and $tRNA^{fMet}$ is derived from interaction with the anticodon stem–loop domain. This result is consistent with the anticodon of $tRNA^{Met}$ being a major specificity determinant for MetRS (Saks et al., 1994). For example, change of the UAC anticodon of $tRNA^{Val}$ to the CAU anticodon of $tRNA^{Met}$ switches the specificity of aminoacylation of $tRNA^{Val}$ from valine to methionine (Schulman & Pelka, 1988).

Considering that the C-terminal domain had native-like characteristics, we wanted to determine whether it could interact with $tRNA^{Met}$, and, if so, whether that interaction was recapitulated with the anticodon stem–loop hairpin alone. The fusion protein MBP–$C_{367-547}$ bound to the anticodon stem–loop structure with a dissociation constant of 39 ± 5 μM (Figure 5B and Table 1). This affinity is similar to that of $MetRS_{1-547}$ for the anticodon stem–loop hairpin (Table 1). In addition, we obtained enough of the free domain $C_{367-547}$ to show that its complex with the anticodon stem–loop structure was essentially the same (K_d = 31 ± 2 μM) as that of the MBP–$C_{367-547}$ fusion protein (data not shown). By the criterion of RNA binding, therefore, domain $C_{367-547}$ recapitulates the interaction of $MetRS_{1-547}$ for the anticodon stem–loop of $tRNA^{fMet}$.

To determine whether the interaction observed in these gels was specific to the anticodon trinucleotide, we investigated the hairpin stem–loop structure with a GAU instead of a CAU anticodon trinucleotide sequence. $MetRS_{1-547}$ binding was weak and MBP–$C_{367-547}$ binding was not detectable to the mutant anticodon stem–loop that contains the anticodon GAU instead of the wild-type anticodon CAU (Figure 5C and Table 1). This experiment established that domain $C_{367-547}$ maintains the same specificity as $MetRS_{1-547}$ for interaction with the RNA substrates. Because this specificity duplicates the specificity of interaction seen between MetRS and $tRNA^{Met}$ (Schulman & Pelka, 1983), we believe that MBP–$C_{367-547}$ is binding to the RNA substrates in a native orientation.

DISCUSSION

Methionyl tRNA synthetase from *Thermus thermophilus* has been analyzed structurally by limited proteolysis. *T.*

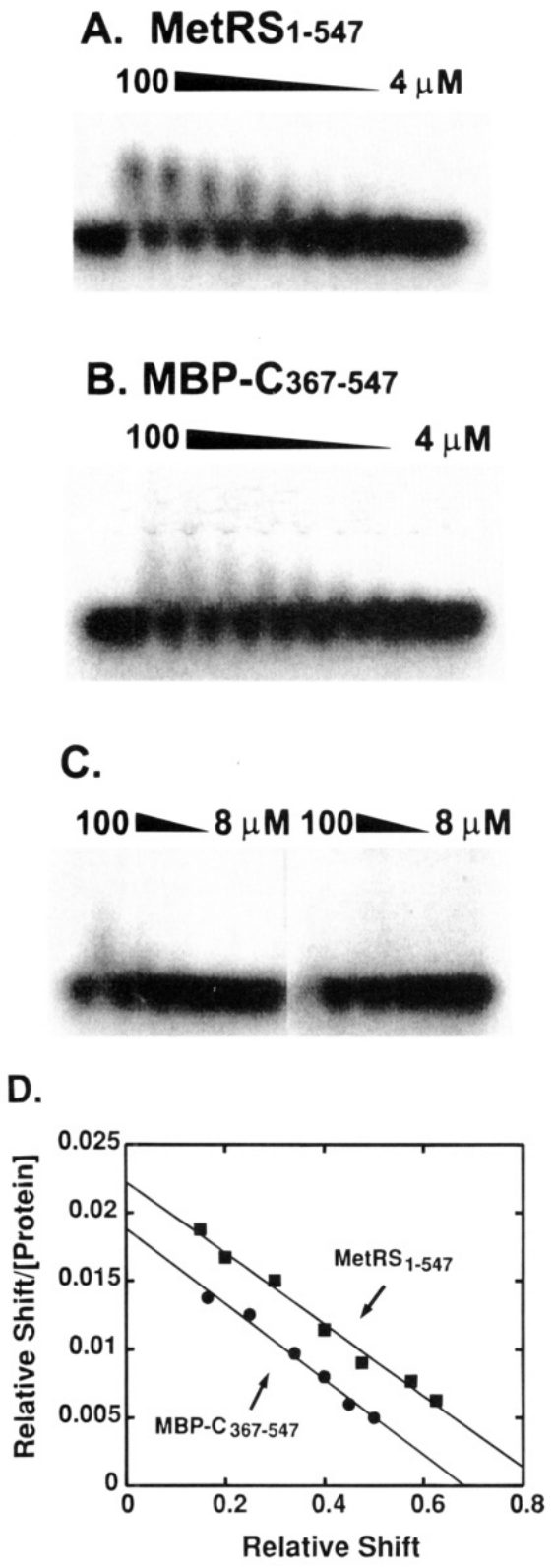

FIGURE 5: Affinity coelectrophoresis gel analysis of the binding of $MetRS_{1-547}$ and $MBP-C_{367-547}$ to the $tRNA^{fMet}$ anticodon stem−loop RNA hairpins. (A) ACE gel of $MetRS_{1-547}$ with the wild-type anticodon stem−loop RNA hairpin ($MetRS_{1-547}$ concentration ranged from 4 to 100 μM). (B) ACE gel of $MBP-C_{367-547}$ with the wild-type CAU anticodon stem−loop RNA hairpin ($MBP-C_{367-547}$ concentration ranged from 4 to 100 μM). (C) ACE gels of $MetRS_{1-547}$ (left) and $MBP-C_{367-547}$ (right) with the GAU anticodon mutant of the anticodon stem−loop RNA hairpin (concentration ranged from 8 to 100 μM for both proteins). (D) Scatchard plots of the binding of $MetRS_{1-547}$ and $MBP-C_{367-547}$ to the anticodon stem−loop RNA hairpin.

Table 1: Dissociation Constants of $MetRS_{1-547}$ and $MBP-C_{367-547}$ for the Anticodon Stem−Loop RNA Substrate at pH 7.5 and 25 °C[a]

	dissociation constant K_d (μM)	
protein	CAU (wild-type)	GAU
$MetRS_{1-547}$	31[b] ± 5	*e*
$MBP-C_{367-547}$	39[c] ± 5	not detectable
$C_{367-547}$	31[d] ± 2	not detectable
MBP	not detectable	not tested

[a] The anticodon stem−loop substrate was chemically synthesized with a sequence according to that of $tRNA^{fMet}$ (Figure 1). [b] Average of two determinations given in Kim et al. (1993b) and of a single determination made in this work. [c] Average of five determinations made in this work. [d] Average of two determinations made in this work. The K_d values were determined from a Scatchard plot of the data obtained from affinity coelectrophoresis (see Materials and Methods and Figure 5). [e] Weak binding to the GAU anticodon substrate was detected for $MetRS_{1-547}$, but the gel shift was smeared, making calculation of the K_d difficult. One possible explanation for a weak interaction that produced a smear in the gel is a nonspecific interaction with the tRNA acceptor stem binding site that is located in the N-terminal domain.

thermophilus MetRS was cleaved into four stable domains, designated T1−T4, in order of their location from the N-terminal to C-terminal end of the protein (Kohda et al., 1987). T1, but not T2, is active in aminoacylation, whereas both T1 and T2 could be cross-linked to $tRNA^{Met}$. These two domains appear to correspond to the N-terminal catalytic domain and the C-terminal anticodon binding domain of *E. coli* MetRS, respectively.

Although the catalytic domain is shared by all enzymes in the same class, insertions into that domain and the second major domain are idiosyncratic to the enzyme (Starzyk et al., 1987; Schimmel et al., 1993). For example, the second domain of class I methionyl tRNA synthetase is comprised of α-helices (Brunie et al., 1990), while the corresponding domain of the related class I glutaminyl tRNA synthetase is rich in β-structure (Rould et al., 1989, 1991). Moreover, in comparing sequences of a particular tRNA synthetase through evolution, the class-defining catalytic domain is much more strongly conserved than is the second domain. Thus, the class I *E. coli* and human isoleucyl tRNA synthetases have a 16−20% similarity of sequence throughout the N-terminal catalytic domain, but the C-terminal domain shows a similarity of only 0−7%, depending on the region of the domain that is considered (Shiba et al., 1994).

The primordial tRNA synthetases probably lacked these idiosyncratic domains, and were most likely comprised of the class-defining catalytic domains that could activate amino acids. When bound to an RNA substrate, these small enzymes may have interacted with no more than a few nucleotides adjacent to the amino acid attachment site. These RNA substrates possibly resembled the acceptor−TΨC minihelix domain of contemporary tRNAs (Schimmel et al., 1993). In the case of the class II alanyl tRNA synthetase, a fragment comprising approximately half of the enzyme has been directly demonstrated to aminoacylate the minihelix domain of $tRNA^{Ala}$ (Buechter & Schimmel, 1993b). With *E. coli* methionyl tRNA synthetase, anticodon interactions are mediated through a helix−loop motif that encompasses W461 of the C-terminal domain (Ghosh et al., 1990, 1991; Kim et al., 1993a; Auld & Schimmel, 1995). Deletion of 11 amino acids from this motif eliminates interaction with the anticodon of $tRNA^{Met}$, but has no effect on the activity for amino acid activation or on that for aminoacylation of a

microhelix comprised of the seven base pairs of the $tRNA^{Met}$ acceptor stem (Kim & Schimmel, 1992). Thus, the capacity of the core enzyme for amino acid activation or aminoacylation of an acceptor stem substrate is not dependent on the integrity of the second domain.

The present work shows that, conversely, the anticodon binding function of the second domain of at least methionyl tRNA synthetase acts independently of the catalytic domain. We found no evidence for domain−domain cooperativity, at least with respect to the binding of the anticodon stem−loop structure. Our data do not address the question of whether domain−domain interactions at the subunit interface affect the energy of the transition state for aminoacylation (k_{cat}) through subtle conformational effects at the active site. However, because deletion of the helix−loop motif that binds the anticodon does not affect the activity for microhelix aminoacylation (Kim & Schimmel, 1992), we surmise that any domain−domain communication may require an intact tRNA "bridge" that spans across the two structural units. A similar suggestion was made by Wright et al. (1993) in their analysis of interactions of *E. coli* GlnRS with the acceptor stem helix and anticodon stem−loop domain of $tRNA^{Gln}$.

The C-terminal end of MetRS is an appendix that extends back to the catalytic site (Brunie et al., 1990), where it contributes to binding of the acceptor stem of $tRNA^{Met}$ (Kim et al., 1993b). We thought that this contact might influence the conformation of the anticodon binding domain and that it might also be needed for its stability. However, the affinity for the anticodon hairpin stem−loop of the free C-terminal domain (and of the C-terminal domain $C_{367-547}$ joined to MBP) is comparable to that of $C_{367-547}$ joined to the N-terminal domain of MetRS (Table 1). We conclude that interactions of the C-terminal peptide appendix of MetRS with the N-terminal domain do not affect the RNA binding conformation of domain $C_{367-547}$. This result is consistent with those of Kim et al. (1993b), who showed that a point mutation in the peptide appendix of MetRS (which disrupted acceptor helix contacts) did not affect anticodon binding. In addition, the stability of domain $C_{367-547}$ in isolation is greater than that of MetRS (Figure 4B). The higher thermal stability of domain $C_{367-547}$ compared to MetRS (Figure 4B) shows that interactions of the C-terminal peptide appendix with the catalytic site are not required for the stable, native structure formed by domain $C_{367-547}$.

Because the anticodon binding domain of methionyl tRNA synthetase functions independently of the protein to which it is joined, such as MBP, we imagine that this functional RNA binding unit could be joined to the catalytic core of other tRNA synthetases and then adapted to the particular anticodon-containing tRNA domain of the cognate tRNA. Consistent with this view, recent experiments of Auld and Schimmel (1995) showed that a variant of the anticodon binding helix−loop peptide motifs of IleRS and MetRS could be swapped between the two enzymes, with anticodon binding being switched by a single amino acid swap. In addition to isoleucyl tRNA synthetase, the class I cysteinyl, leucyl, and valyl tRNA synthetases are closely related to methionyl tRNA synthetase, and the structures of these enzymes can be modeled after that of the methionine enzyme (Burbaum et al., 1990; Burbaum & Schimmel, 1991b; Eriani et al., 1991; Hou et al., 1991; Shepard et al., 1992). In spite of the large size variations among these five class I enzymes, and in contrast to the less related class I glutaminyl tRNA synthetase, sequence comparisons of their C-terminal domains suggest that, while highly diverged in sequence, all are made up of α-helices and probably originated from the same progenitor (Shiba & Schimmel, 1992). Thus, the properties of the anticodon binding domain of methionyl tRNA synthetase investigated here may be prototypical of this particular domain in this subclass of tRNA synthetases.

REFERENCES

Auld, D. S., & Schimmel, P. (1995) *Science 267*, 1994−1996.

Brunie, S., Zelwer, C., & Risler, J.-L. (1990) *J. Mol. Biol. 216*, 411−424.

Buechter, D. D., & Schimmel, P. (1993a) *Crit. Rev. Biochem. Mol. Biol. 28*, 309−322.

Buechter, D. D., & Schimmel, P. (1993b) *Biochemistry 32*, 5267−5272.

Burbaum, J. J., & Schimmel, P. (1991a) *Biochemistry 30*, 319−324.

Burbaum, J. J., & Schimmel, P. (1991b) *J. Biol. Chem. 266*, 16965−16968.

Burbaum, J. J., Starzyk, R. M., & Schimmel, P. (1990) *Proteins: Struct. Funct., Genet. 7*, 99−111.

Cantor, C. R., & Schimmel, P. R. (1980a) *Biophysical Chemistry Part II: Techniques for the Study of Biological Structure and Function*, W. H. Freeman and Company, San Francisco.

Cantor, C. R., & Schimmel, P. R. (1980b) *Biophysical Chemistry Part III: The Behavior of Biological Macromolecules*, W. H. Freeman and Company, San Francisco.

Cassio, D., & Waller, J.-P. (1971) *Eur. J. Biochem. 20*, 283−300.

Cavarelli, J., Rees, B., Ruff, M., Thierry, J.-C., & Moras, D. (1993) *Nature 362*, 181−184.

Cusack, S., Berthet-Colominas, C., Härtlein, M., Nassar, N., & Leberman, R. (1990) *Nature 347*, 249−255.

Edelhoch, H. (1967) *Biochemistry 6*, 1948−1954.

Eriani, G., Delarue, M., Poch, O., Gangloff, J., & Moras, D. (1990) *Nature 347*, 203−206.

Eriani, G., Dirheimer, G., & Gangloff, J. (1991) *Nucleic Acids Res. 19*, 265−269.

Ghosh, G., Pelka, H., & Schulman, L. H. (1990) *Biochemistry 29*, 2220−2225.

Ghosh, G., Kim, H. Y., Demaret, J.-P., Brunie, S., & Schulman, L. H. (1991) *Biochemistry 30*, 11767−11774.

Guan, C., Li, P., Riggs, P. D., & Inouye, H. (1987) *Gene 67*, 21−30.

Hou, Y.-M., Shiba, K., Mottes, C., & Schimmel, P. (1991) *Proc. Natl. Acad. Sci. U.S.A. 88*, 976−980.

Hountondji, C., Dessen, P., & Blanquet, S. (1986) *Biochimie 68*, 1071−1078.

Kim, S., & Schimmel, P. (1992) *J. Biol. Chem. 267*, 15563−15567.

Kim, H. Y., Pelka, H., Brunie, S., & Schulman, L. H. (1993a) *Biochemistry 32*, 10506−10511.

Kim, S., Landro, J. A., Gale, A. J., & Schimmel, P. (1993b) *Biochemistry 32*, 13026−13031.

Kohda, D., Yokoyama, S., & Miyazawa, T. (1987) *J. Biol. Chem. 262*, 558−563.

Lee, M. K., & Lander, A. D. (1991) *Proc. Natl. Acad. Sci. U.S.A. 88*, 2768−2772.

Lim, W. A., Sauer, R. T., & Lander, A. D. (1991) *Methods Enzymol. 208*, 196−210.

Ludmerer, S. W., & Schimmel, P. (1987) *J. Biol. Chem. 262*, 10801−10806.

Maina, C. V., Riggs, P. D., Grandea, A. G. I., Slatko, B. E., Moran, L. S., Tagliamonte, J. A., McReynolds, L. A., & Guan, C. (1988) *Gene 74*, 365−373.

Maizels, N., & Weiner, A. M. (1993) in *The RNA World* (Gesteland, R. F., & Atkins, J. F., Eds.) pp 577−602, Cold Spring Harbor Laboratory Press, Cold Spring Harbor, NY.

Meinnel, T., Mechulam, Y., Blanquet, S., & Fayat, G. (1991a) *J. Mol. Biol. 220*, 205−208.

Meinnel, T., Mechulam, Y., Le Corre, D., Panvert, M., Blanquet, S., & Fayat, G. (1991b) *Proc. Natl. Acad. Sci. U.S.A. 88*, 291−295.

Musier-Forsyth, K., Scaringe, S., Usman, N., & Schimmel, P. (1991) *Proc. Natl. Acad. Sci. U.S.A. 88*, 209−213.
Noller, H. F. (1993) in *The RNA World* (Gesteland, R. F., & Atkins, J. F., Eds.) pp 137−156, Cold Spring Harbor Laboratory Press, Cold Spring Harbor, NY.
Park, S. J., & Schimmel, P. (1988) *J. Biol. Chem. 263*, 16527−16530.
Perona, J. J., Rould, M. A., Steitz, T. A., Risler, J.-L., Zelwer, C., & Brunie, S. (1991) *Proc. Natl. Acad. Sci. U.S.A. 88*, 2903−2907.
Rould, M. A., Perona, J. J., Söll, D., & Steitz, T. A. (1989) *Science 246*, 1135−1142.
Rould, M. A., Perona, J. J., Söll, D., & Steitz, T. A. (1991) *Nature 352*, 213−218.
Saks, M. E., Sampson, J. R., & Abelson, J. N. (1994) *Science 263*, 191−197.
Sambrook, J., Fritsch, E. F., & Maniatis, T. (1989) *Molecular Cloning: A Laboratory Manual*, Cold Spring Harbor Laboratory Press, Cold Spring Harbor, NY.
Scaringe, S. A., Francklyn, C., & Usman, N. (1990) *Nucleic Acids Res. 18*, 5433−5441.
Schimmel, P., Giegé, R., Moras, D., & Yokoyama, S. (1993) *Proc. Natl. Acad. Sci. U.S.A. 90*, 8763−8768.
Schulman, L. H., & Pelka, H. (1983) *Proc. Natl. Acad. Sci. U.S.A. 80*, 6755−6759.
Schulman, L. H., & Pelka, H. (1988) *Science 242*, 765−768.
Shepard, A., Shiba, K., & Schimmel, P. (1992) *Proc. Natl. Acad. Sci. U.S.A. 89*, 9964−9968.
Shiba, K., & Schimmel, P. (1992) *Proc. Natl. Acad. Sci. U.S.A. 89*, 1880−1884.
Shiba, K., Suzuki, N., Shigesada, K., Namba, Y., Schimmel, P., & Noda, T. (1994) *Proc. Natl. Acad. Sci. U.S.A. 91*, 7435−7439.
Silberklang, M., Gillum, A. M., & Rajbhandary, U. L. (1977) *Nucleic Acids Res. 4*, 4091−4108.
Sprinzl, M., Hartmann, T., Weber, J., Blank, J., & Zeidles, R. (1989) *Nucleic Acids Res. 17*, r1−r172.
Starzyk, R. M., Webster, T. A., & Schimmel, P. (1987) *Science 237*, 1614−1618.
Usman, N., Ogilvie, K. K., Jiang, M.-Y., & Cedergren, R. J. (1987) *J. Am. Chem. Soc. 109*, 7845−7854.
Valenzuela, D., & Schulman, L. H. (1986) *Biochemistry 25*, 4555−4561.
Webster, T. A., Tsai, H., Kula, M., Mackie, G. A., & Schimmel, P. (1984) *Science 226*, 1315−1317.
Wright, D. R., Martinis, S. A., Jahn, M., Söll, D., & Schimmel, P. (1993) *Biochimie 75*, 1041−1049.

BI950685T